PHYSICAL REVIEW B **94**, 220103(R) (2016)

Unidirectional single-photon generation via matched zero-index metamaterials

Jingping Xu,[1,2] Ge Song,[1] Zhenqing Zhang,[1] Yaping Yang,[1,*] Hong Chen,[1] M. Suhail Zubairy,[2,3] and Shiyao Zhu[2,4,†]

[1] *MOE Key Laboratory of Advanced Micro-Structured Materials, School of Physics Science and Engineering, Tongji University, Shanghai 200092, People's Republic of China*

[2] *Beijing Computational Science Research Center, Beijing 100084, People's Republic of China*

[3] *Institute for Quantum Science and Engineering (IQSE) and Department of Physics and Astronomy, Texas A&M University, College Station, Texas 77843-4242, USA*

[4] *Department of Physics, Zhejiang University, Hangzhou 310027, People's Republic of China*

(Received 3 February 2016; revised manuscript received 14 November 2016; published 8 December 2016)

We propose a scheme which can generate a highly directional single photon with almost 100% efficiency. Therefore we can get a useful single photon when it is required. An initial excited atom is placed inside a special Fabry-Pérot cavity whose walls consist of left-handed and zero-index metamaterials. The left-handed slabs work as a closed shell to avoid dissipation of the emitted photon, while the outer zero-index metamaterial slabs act as a special shutter which is transparent only for normal incidence, so that the photon emitted by the atom can only escape out of the cavity unidirectionally. Furthermore, we design the cavity with currently available metamaterials made of two-dimensional dielectric photonic crystals, and simulate the radiative field of an electric dipole to confirm our prediction. Differently from the previous proposal of single-photon sources which demanded complicated structure design and subtle mode analysis, our scheme is simple and robust for atomic position. This work has promising applications for quantum communication and optical quantum computing.

DOI: 10.1103/PhysRevB.94.220103

Sources of single photons are indispensable elements in quantum information science [1]. In particular, they pave the way to approach quantum computing [2], quantum communications [3], and especially quantum encryption technologies [4]. The most prominent single-photon source is the fluorescent light from a single two-level system. Therefore tremendous progress has been made based on single molecules [5], semiconductor quantum dots [6], and single nitrogen vacancy centers in diamond [7]. Recently, single-photon sources based on WSe_2 atomic layers have also been reported [8].

There are two factors to judge the quality of single-photon sources, namely, the repetition rate and the collimation of the photon. Among them the collimation happens to be a huge challenge. It is known that the radiation of a two-level system in free space spreads over almost 4π solid angle and its propagation direction cannot be predicted for certain emission events. To overcome this impediment, there are two possible ways. The first way resorts to the surface plasmon [9,10], because an excited plasmon can only propagate near the surface of metal. However the shortcoming of the plasmon is apparent as it cannot propagate over several wavelengths because of huge losses. Therefore, many kinds of hybrid plasmon nanostructures [11–14] are suggested to excite the plasmon at first and then transfer it into guided modes through another high-index dielectric waveguide. However the quantum efficiency of these hybrid systems is low because of the double transformation, i.e., from atom to plasmon and from plasmon to photon. An alternative way is to generate a propagating single photon directly through carefully designed microstructures. A pillar microcavity [15], photonic crystal structures [16], carbon nanotubes [17], optical antennas [18], and multilayered hyperbolic metamaterials [19] have been proposed as candidates to control the directionality of the emitted photon. However it is difficult to maintain the unidirectional emission and the high quantum efficiency at the same time. In addition, both methods (plasmon and propagating photon) require complicated structure design, subtle mode analysis, and optimized position of emitter to make sure that the atom can mainly excite the wanted mode, which is quite challenging.

In this Rapid Communication, we propose a kind of cavity made by metamaterials in which an excited two-level atom can generate the unidirectional propagating photon with high efficiency. Here the high efficiency not only refers to the quantum efficiency which is defined by the ratio of radiation emission to the total emission, but also refers to the ratio of unidirectional emission to total emission. More importantly, this scheme does not rely on any mode analysis and is independent of atomic position. The metamaterials mentioned here include the left-handed materials (LHMs) and the zero-index materials (ZIMs). The LHMs refer to the manmade materials possessing effective negative permittivity and negative permeability simultaneously, which demonstrate negative refraction and phase compensation [20]. Meanwhile, the indexes of the ZIMs are almost zero at the frequency of interest. The ZIMs can be used to tailor the radiation phase patterns [21], to squeeze electromagnetic waves [22], and to realize cloaking [23] and Dirac-cone-like dispersions [24,25]. These two kinds of metamaterials are already realized for visible light [26] in experiment.

The scheme and the coordinate system are shown in Fig. 1. The atom (marked by a short arrow) with transition frequency ω_0 is placed in the empty cavity at position $\boldsymbol{r}_a = (0,0,z_a)$. It can be excited with a pump field propagating along the y axis. The wall of the cavity is the combination of the LHM and

*Corresponding author: yaping_yang@tongji.edu.cn

†Corresponding author: syzhu@csrc.ac.cn

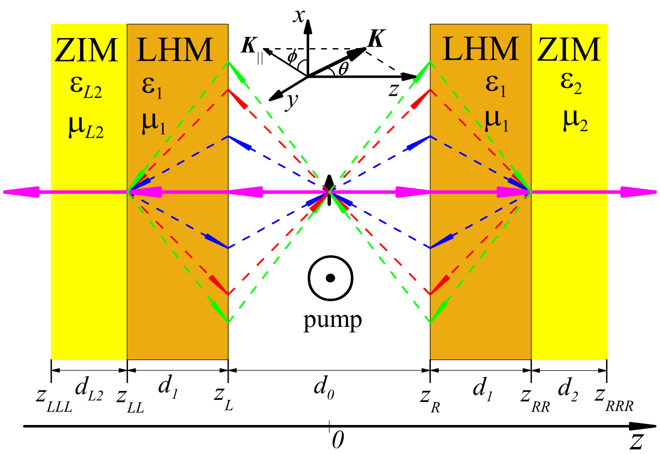

FIG. 1. The geometric optical path of the radiative field emitted by an atom (short black arrow) in the cavity made of LHMs and ZIMs.

ZIM slabs. The LHM slabs possess indexes of $\varepsilon_1 = \mu_1 = -1$ and the thickness d_1. Their unique characteristic of negative refraction is demonstrated by the geometric optical arrows in Fig. 1. With the choice of $d_0 = 2d_1$, two LHM slabs act as the enclosed shell to avoid the escape of atomic emission field along x-y plane if the outer boundary of the LHM can totally reflect the field. The unidirectional single photon will be generated if we can find a special filter which is transparent only for horizontal incidence but totally reflective for others. The metal is unqualified because it reflects all the incident fields. A suitable candidate is the ZIM slab. It has been proved that, at the interface between the vacuum and the ZIM ($\varepsilon_2 = \mu_2 = 0$), reflection coefficients for both TE and TM polarizations are equal to -1 for oblique incidence, but are zero for normal incidence [27]. Thus, employing the unique characteristics of LHMs and ZIMs, the spontaneous decay of the atom can generate a highly directional single photon.

In a highly accessible language, the principle is that the photon emitted obliquely will trace back to the atom and interact with it again. The photon is scattered again into arbitrary directions. This cycle continues until the photon is emitted into the horizontal direction and then it can escape out of the cavity and be used as a single photon. Such straightforward generation of a unidirectional single photon is similar to squeezing toothpaste out of a tube. The advantages of such a scheme for a single-photon source are obvious. First, the mode analysis is not required as the waveguide modes and surface plasmon modes can be ignored here since the atom is away from the interfaces. Second, the unidirectional single-photon generation is independent of atomic position. The optical path in Fig. 1 is just an example of the atom being in the center. The radiative field can still trace back to the atom even if the atom is located at other positions. Third, the efficiency of generation of the unidirectional photon is high because, even if the photon is initially emitted into an arbitrary direction, it can only leak out of the cavity in the horizontal direction. This means that once the two-level atom is excited, a single photon can be collected along the z axis deterministically, leading to a superior design for a highly directional single-photon emitter.

The above analysis is based on the classical optical path. In the following we calculate the atomic spontaneous emission field to confirm our prediction. Starting with an initial state in which the atom is in the excited state and the electromagnetic field is in the vacuum state, the intensity of the single-photon emission field is given by the first-order correlation function [28]

$$|\boldsymbol{E}(\boldsymbol{r},t)|^2 = \langle\psi(t)|\hat{\boldsymbol{E}}^+(\boldsymbol{r},t)\cdot\hat{\boldsymbol{E}}(\boldsymbol{r},t)|\psi(t)\rangle = |\langle 0|\hat{\boldsymbol{E}}(\boldsymbol{r},t)|\gamma_0(t)\rangle|^2, \tag{1}$$

where $|\gamma_0(t)\rangle$ represents the state of the electromagnetic field. After a lengthy calculation similar to that given in Refs. [9,29], we obtain

$$\langle 0|\hat{\boldsymbol{E}}(\boldsymbol{r},t)|\gamma_0(t)\rangle = i\frac{C_u(t)}{\varepsilon_0}\frac{\omega_0^2}{c^2}e^{-i\omega_0 t}\mathrm{Im}\overset{\leftrightarrow}{\boldsymbol{G}}(\boldsymbol{r},\boldsymbol{r}_a,\omega_0)\cdot\boldsymbol{P}_a. \tag{2}$$

Here $C_u(t)$ is the probability amplitude of the atom in the excited state. It follows that the evolution under the Markovian approximation is given by [9,30]

$$\dot{C}_u(t) = -\frac{1}{2}C_u(t)\left(\frac{2}{\varepsilon_0\hbar}\frac{\omega_0^2}{c^2}\boldsymbol{P}_a\cdot\mathrm{Im}\overset{\leftrightarrow}{\boldsymbol{G}}(\boldsymbol{r}_a,\boldsymbol{r}_a,\omega_0)\cdot\boldsymbol{P}_a\right) = -\frac{1}{2}\Gamma C_u(t), \tag{3}$$

where $\boldsymbol{P}_a$ is the atomic dipole momentum, $\mathrm{Im}\boldsymbol{G}(\boldsymbol{r},\boldsymbol{r}_a,\omega_0)$ is the imaginary part of the electromagnetic Green's tensor at the transition frequency ω_0, and Γ is the atomic spontaneous decay rate. The Green's tensor required here is shown in the Supplemental Material [31].

We describe the spatial radiative field with the normalized expectation value of the electric field $|E(r,t)|/E_0(t)$where $E_0(t) = p_a\omega_0^3|C_u(t)|/(8\pi c^3)$. The normalized field is time-independent and exhibits a clear spatial pattern. The atomic dipole momentum is set to be parallel to the interface, i.e., $\boldsymbol{P}_a = P_a\hat{\boldsymbol{x}}$. The length of the cavity is chosen as $d_0 = 4\lambda_0$. For the LHM slabs, $\varepsilon_1 = \mu_1 = -1$ and their thickness is $d_1 = 2\lambda_0$. Meanwhile the ZIM slabs possesses $\varepsilon_{L2} = \mu_{L2} = \varepsilon_2 = \mu_2 = 0.1$ and $d_{L2} = d_2 = \lambda_0$. The atomic radiative field distribution in the x-z plane is plotted in Fig. 2(a).

It is obvious that LHM slabs can trap the atomic emission field, and refocus them at three positions which agree with the geometrical optics result shown in Fig. 1. The electric field attenuates quickly with the penetration from the LHM slab into the ZIM slab. When the field escapes out of the ZIM, most of it just propagates normal to the interface. The corresponding far-field radiation patterns are plotted in Fig. 2(b) which is defined through the field intensity at the distance 30λ away from the origin. It is clear that the photon can only escape out of the cavity within a narrow radiative angle, namely less than 10°, which is good enough for most applications. Although we only plot the field distribution in the x-z plane, the property of unidirectional emission remains for any rotated plane around the z axis.

Although the atomic decay rate in our scheme is low, i.e., $\Gamma = 0.024\Gamma_0$, we can show that such small decay rate just originates from the electromagnetic modes escaping out of the ZIM slab, while the electromagnetic modes cycling inside the cavity have no contribution to the decay rate. The decay rate

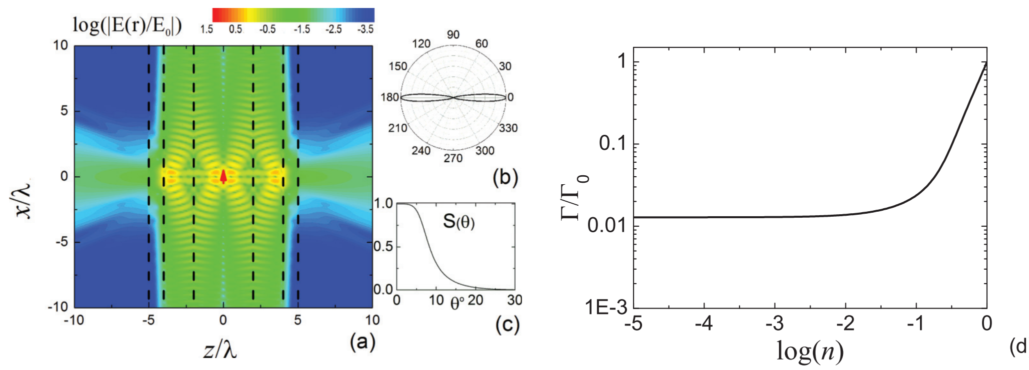

FIG. 2. (a) The radiated electric field distribution in the x-z plane, (b) the far-field radiative pattern, and (c) the angular spectrum of the decay rate when the atom is in the cavity with parameters $\varepsilon_1 = \mu_1 = -1$, $\varepsilon_{L2} = \mu_{L2} = \varepsilon_2 = \mu_2 = 0.1$, $d_1 = 2\lambda_0$, $d_{L2} = d_2 = \lambda$. (d) The decay rate as function of the index of ZIM with the definition $\varepsilon_2 = \mu_2 = \varepsilon_{L2} = \mu_{L2} = n$.

is given by

$$\Gamma = \frac{2}{\varepsilon_0\hbar}\frac{\omega_0^2}{c^2}\boldsymbol{P}_a\cdot \mathrm{Im}\overleftrightarrow{\boldsymbol{G}}(\boldsymbol{r}_a,\boldsymbol{r}_a,\omega_0)\cdot\boldsymbol{P}_a$$
$$= \frac{3}{4}\Gamma_0\int d\theta\,\sin\theta\, S(\theta). \quad (4)$$

Here $\Gamma_0 = P_a^2\omega_a^3/(3\pi\varepsilon_0\hbar c^3)$ is the decay rate in the free space and $S(\theta)$ is the angular spectrum of the decay rate which describes the contributions of these modes possessing wave vectors with azimuthal angle θ as defined in Fig. 1 (note that it has been integrated over polar angle Φ already). The corresponding angular spectra $S(\theta)$ are shown in Fig. 2(c). It is clear that the FWHW of $S(\theta)$ is 8^{o} which fits to the beam shape in Fig. 2(a). Although the decay rate is low, the emission energy of the atom completely transfers into the unidirectional propagating photon, which corresponds to nearly 100% transformation efficiency.

To explore the influence of ZIM on the decay rate, we plot the decay rate as a function of the index of ZIM, $\varepsilon_2 = \mu_2 = \varepsilon_{L2} = \mu_{L2} = n$, in Fig. 2(d). Other parameters are the same as those in Fig. 2(a). It shows that when the index of ZIM falls into the region $n \in [10^{-5},10^{-2}]$, the atomic decay rate is nearly a constant, i.e., $\Gamma \approx 0.013\Gamma_0$. However when n is increased further, the decay rate monotonically increases accordingly. The decay rate reaches to $0.1\Gamma_0$ when $n = 10^{-0.5}$. A reasonable estimate leads to the conclusion that the unidirectional emission of the single photon is valid for a wider region of the index of the ZIM, i.e., $n \in (0,10^{-0.5}]$.

For the above symmetrical cavity, the photon can escape out in both directions. To improve the unidirectional property, we replace the left ZIM slab (labeled by "L2") by a perfect magnetic conducting (PMC) slab with $\varepsilon_{L2} = 1, \mu_{L2} = -50$, and then the photon can only escape out to the right. The corresponding field distribution and far-field radiation pattern are shown in Fig. 3(a). Comparing Fig. 3(a) with the symmetric case of Fig. 2(a), the radiative field now only leaks out to the right and the unidirectional emission remains. In addition, the field distributions both inside and outside of the cavity as well as the far-field pattern are nearly unchanged. This is the reason why we adopt the PMC (not metal) to block the left port. If we use the metal slab, the atomic decay rate will be deeply inhibited to nearly $10^{-4}\Gamma_0$, and then not only the intracavity field intensity but also the output intensity are greatly attenuated. Instead, the decay rate in the case of the PMC slab, as shown in Fig. 3(a), is increased to $0.04\Gamma_0$ which is double that in Fig. 2(a) with $0.024\Gamma_0$. Such

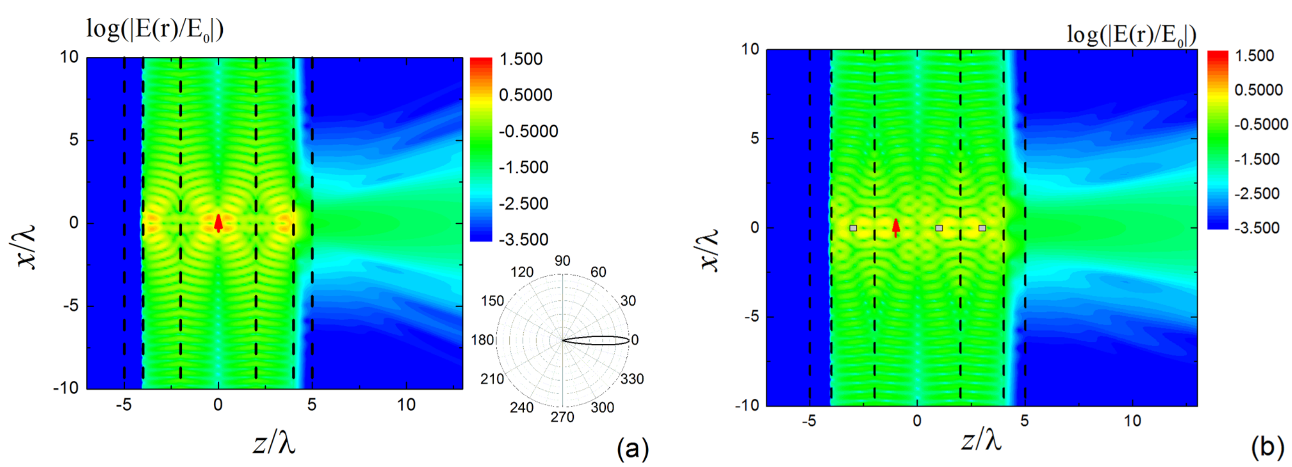

FIG. 3. The atomic radiated electric field distribution in the asymmetric structure. The left slab is replaced by PMC with $\varepsilon_{L2} = 1, \mu_{L2} = -50$. (a) The atom is located at $\boldsymbol{r}_a = (0,0,0)$; (b) the atom is located at $\boldsymbol{r}_a = (0,0,-\lambda)$. Other parameters are the same as those in Fig. 2(a). The inset of (a) is the corresponding far-field radiation pattern.

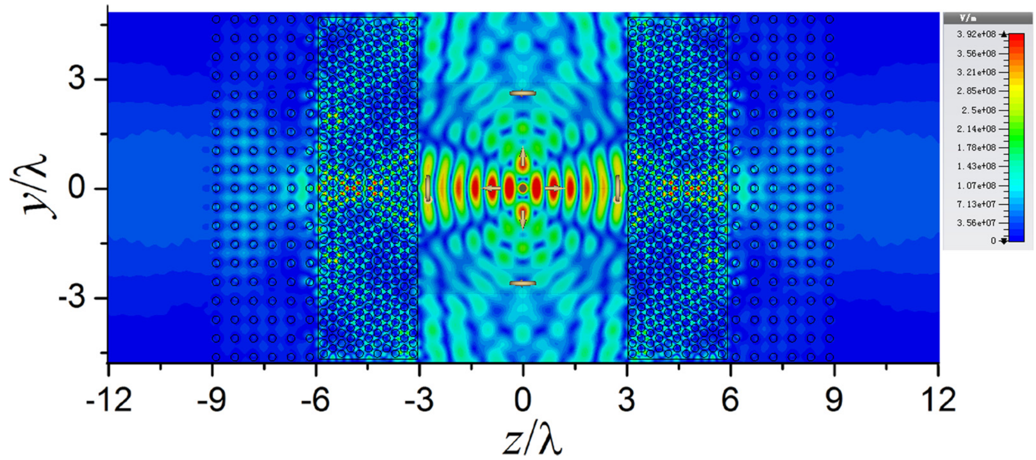

FIG. 4. The field intensity distribution of an oscillating electric dipole located in the cavity made of realistic LHM (enclosed by rectangle) and ZIM which is constructed by a two-dimensional photonic crystal. The detail parameters are presented in the text. The operating wavelength is $\lambda = 1.55\ \mu$m.

improvement originates from the similar boundary characteristics of the ZIM and PMC for TM polarization under oblique incidence.

As mentioned before, the behavior of our scheme is insensitive to the atomic position. In Fig. 3(b), the atomic position is changed to $\boldsymbol{r}_a = (0,0,-\lambda)$, which is a quarter of the cavity length away from the left inner interface. It is clear that there are four focuses of the radiative field marked by squares in Fig. 3(b) which confirm that the LHM slab can still trap the atomic radiation field. Though atomic position affects the radiation field pattern inside the cavity, the unidirectional emission of the photon remains unchanged. Therefore the unidirectional emission of the single photon still works no matter where the atomic position is. The single photon emitted in our scheme is not a plane wave, but a transversely finite beam. For further discussion on the interaction of the generated single photon with a particle outside the cavity, the formulation of the interaction of light with matter in $\boldsymbol{b}$ space [32] can be adopted.

As most metamaterials are made of metal resonators [26], the absorption of the metamaterials cannot be ignored in general. However, if metamaterials are made of the dielectric microstructure, their losses can be neglected. Following Refs. [24,33], we design the effective LHMs and ZIMs through the dielectric two-dimensional photonic crystal working at the operating wavelength $\lambda = 1.55\ \mu$m. The effective LHMs are constructed by a hexagonal lattice (with lattice constant $a_1 = 482$ nm) of circular air holes (with radius $r_1 = 0.365a_1$) drilled in dielectric substrates with permittivity $\varepsilon_m = 10.6$, while the effective ZIMs are constituted by a square lattice (with lattice constant $a_2 = 875$ nm) of dielectric cylinders (with radius $r_2 = 175$ nm and permittivity $\varepsilon = 12.5$). The scheme is shown in Fig. 4, and the plane is defined as the y-z plane. The length in y axis is set as 24λ in simulation with open boundary which is quadruple d_0. Such finite structure implies that the emission for the azimuthal angle above 75° will dissipate out of the cavity. Of course, the structure can be extended in the y axis to reduce the dissipation further. We arrange an oscillating electric dipole normal to the plane with wavelength $\lambda = 1.55\ \mu$m at the middle of the whole structure, and calculate its radiative field intensity distribution, see Fig. 4, using commercial electromagnetic software (CST). As predicted, the radiative field converges at three points; one is the atomic position and the other two are near the boundaries between LHM and ZIM, which is the demonstration of the behavior of the LHMs. Outside of the cavity two beams escape out of the cavity along the horizontal axis, which confirms the effect of the ZIMs.

The anisotropy of the effective LHM slab deserves to be discussed. Though the effective index could be equal to -1 for a wide region of wave vectors, we cannot have exactly the isotropic effective medium due to the realistic discrete lattice. Our analysis shows that the isotropy of the LHM no longer holds, when the azimuthal angle falls to 70° to 90°. Such anisotropy could lead to a tiny reflectivity and the nonperfect negative refraction at the interfaces z_L and z_R, (defined in Fig. 1) at the angles from 70° to 90°, which have some influence on the field distribution in the cavity. However, the effective ZIM is robust, which makes sure the unidirectional emission of the single photon out of the cavity. Therefore, the effect of the anisotropy on the unidirectional single-photon generation is small.

In summary, we present a design of a collimated single-photon emitter with high efficiency. The single photon originates from an excited atom located in a special cavity made of manmade left-handed materials and zero-index materials. The scheme to generate the unidirectional single photon is straightforward, which does not need any mode analysis and subtle optimization. In addition, the performance is insensitive to the atomic position. As almost all the atomic energy can be transformed into the unidirectional photon, we can generate a single photon when it is required by simply exciting the atom. The price for the high efficiency is the low repeating rate, because the emission time of each photon is about $50/\Gamma_0$. We also design realistic effective LHMs and ZIMs through two-dimensional dielectric photonic crystals, and our simulations fit well with the theoretical prediction. Such kind of QED system can work as a highly efficient unidirectional single-photon emitter with promising applications in quantum information science.

This research was supported by the National Natural Science Foundation of China (Grants No. 11574229, No. 11474221, No. 11234010, No. 11274242), the Joint Fund of the National Natural Science Foundation of China (Grant No. U1330203), the 973 program (Grants No. 2013CB632701, No. 2016YFA0301101), the Shanghai Science and Technology Committee (Grant No. 15XD1503700) and the Shanghai Education Commission Foundation. M.S.Z is supported by NPRP Grant No. 7-210-1-032 from the Qatar National Research Fund (QNRF).

[1] B. Lounis and M. Orrit, Rep. Prog. Phys. **68**, 1129 (2005).
[2] E. Knill, R. Laflamme, and G. J. Milburn, Nature (London) **409**, 46 (2001).
[3] N. Gisin and R. Thew, Nat. Photonics. **1**, 165 (2007).
[4] N. Gisin, G. Ribordy, W. Tittel, and H. Zbinden, Rev. Mod. Phys. **74**, 145 (2002).
[5] B. Lounis and W. E. Moerner, Nature (London) **407**, 491 (2000).
[6] G.-C. Shan, Z.-Q. Yin, C. H. Shek, and W. Huang, Front. Phys. **9**, 170 (2013); G. Muñoz-Matutano, D. Barrera, C. R. Fernández-Pousa, R. Chulia-Jordan, L. Seravalli, G. Trevisi, P. Frigeri, S. Sales, and J. Martínez-Pastor, Sci. Rep. **6**, 27214 (2016).
[7] C. Kurtsiefer, S. Mayer, P. Zarda, and H. Weinfurter, Phys. Rev. Lett. **85**, 290 (2000); M. Gould, E. R. Schmidgall, S. Dadgostar, F. Hatami, and Kai-Mei C. Fu, Phys. Rev. Appl. **6**, 011001 (2016).
[8] Y.-M. He, G. Clark, J. R. Schaibley, Y. He, M.-C. Chen, Y.-J. Wei, X. Ding, Q. Zhang, W. Yao, X. Xu, C.-Y. Lu, and J.-W. Pan, Nat. Nanotech. **10**, 497 (2015); C. Chakraborty, L. Kinnischtzke, K. M. Goodfellow, R. Beams, and A. N. Vamivakas, *ibid.* **10**, 507 (2015); J. Kern, I. Niehues, P. Tonndorf, R. Schmidt, D. Wigger, R. Schneider, T. Stiehm, S. M. de Vasconcellos, D. E. Reiter, T. Kuhn, and R. Bratschitsch, Adv. Mater. **28**, 7101 (2016).
[9] J.-P. Xu, Y.-P. Yang, and S.-Y. Zhu, J. Mod. Opt. **57**, 1473 (2010).
[10] D. E. Chang, A. S. Sørensen, P. R. Hemmer, and M. D. Lukin, Phys. Rev. Lett. **97**, 053002 (2006).
[11] K. J. Russell, T.-L. Liu, S. Cui, and E. L. Hu, Nat. Photonics **6**, 459 (2012).
[12] X.-W. Chen, M. Agio, and V. Sandoghdar, Phys. Rev. Lett. **108**, 233001 (2012).
[13] G. M. Akselrod, C. Argyropoulos, T. B. Hoang, C. Ciracì, C. Fang, J. Huang, D. R. Smith, and M. H. Mikkelsen, Nat. Photonics **8**, 835 (2014); T. B. Hoang, G. M. Akselrod, and M. H. Mikkelsen, Nano. Lett. **16**, 270 (2016).
[14] H. Lian, Y. Gu, J.-J. Ren, F. Zhang, L.-J. Wang, and Q.-H. Gong, Phys. Rev. Lett. **114**, 193002 (2015).
[15] C. Santori, D. Fattal, J. Vučković, G. S. Solomon, and Y. Yamamoto, Nature (London) **419**, 594 (2002); S. L. Portalupi, G. Hornecker, V. Giesz, T. Grange, A. Lemaître, J. Detmory, I. Sagnes, N. D. Lanzillotti-Kimura, L. Lanco, A. Auffèves, and P. Senellart, Nano. Lett. **15**, 6290 (2015); X. Ding, Y. He, Z.-C. Duan, N. Gregersen, M.-C. Chen, S. Unsleber, S. Maier, C. Schneider, M. Kamp, S. Höfling, C.-Y. Lu, and J.-W. Pan, Phys. Rev. Lett. **116**, 020401 (2016).
[16] M. Toishi, D. Englund, A. Faraon, and J. Vučković, Opt. Express **17**, 14618 (2009).
[17] A. Jeantet, Y. Chassagneux, C. Raynaud, Ph. Roussignol, J. S. Lauret, B. Besga, J. Estève, J. Reichel, and C. Voisin, Phys. Rev. Lett. **116**, 247402 (2016).
[18] A. G. Curto, G. Volpe, T. H. Taminiau, M. P. Kreuzer, R. Quidant, and N. F. van Hulst, Science **329**, 930 (2010); K. G. Lee, X. W. Chen, H. Eghlidi, P. Kukura, R. Lettow, A. Renn, V. Sandoghdar, and S. Götzinger, Nat. Photonics **5**, 166 (2011).
[19] K. V. Sreekanth, T. Biaglow, and G. Strangi, J. Appl. Phys. **114**, 134306 (2013).
[20] J. B. Pendry, Phys. Rev. Lett. **85**, 3966 (2000).
[21] A. Alù, M. G. Silveirinha, A. Salandrino, and N. Engheta, Phys. Rev. B **75**, 155410 (2007).
[22] R. Liu, Q. Cheng, T. Hand, J. J. Mock, T. J. Cui, S. A. Cummer, and D. R. Smith, Phys. Rev. Lett. **100**, 023903 (2008).
[23] V. C. Nguyen, L. Chen, and K. Halterman, Phys. Rev. Lett. **105**, 233908 (2010).
[24] X. Huang, Y. Lai, Z. H. Hang, H. Zheng, and C. T. Chan, Nat. Mater. **10**, 582 (2011).
[25] L.-G. Wang, G.-X. Li, and S.-Y. Zhu, Phys. Rev. B **81**, 073105 (2010).
[26] Y.-X. Zhao, F. Chen, Q. Shen, Q.-W. Liu, and L.-M. Zhang, Opt. Express. **19**, 11605 (2011); P. Moitra, Y. Yang, Z. Anderson, I. I. Kravchenko, D. P. Briggs, and J. Valentine, Nat. Photonics **7**, 791 (2013).
[27] J.-P. Xu, M. Alamri, Y.-P. Yang, S.-Y. Zhu, and M. S. Zubairy, Phys. Rev. A **89**, 053831 (2014).
[28] M. O. Scully and M. S. Zubairy, *Quantum Optics* (Cambridge University Press, 1997), pp. 208-209.
[29] M. S. Tomaš, Phys. Rev. A **51**, 2545 (1995).
[30] H. T. Dung, L. Knoll, and D.-G. Welsch, Phys. Rev. A. **66**, 063810 (2002).
[31] See Supplemental Material at http://link.aps.org/supplemental/10.1103/PhysRevB.94.220103 for the Green's tensor involved.
[32] L. Kaplan and J. H. McGuire, Phys. Rev. A **92**, 032702 (2015).
[33] W. Śmigaj, B. Gralak, R. Pierre, and G. Tayeb, Opt. Lett. **34**, 3532 (2009).